Directors' research and development activities
R & D activities on the structures constructed by the press-in method

Yukihiro Ishihara, Nanase Ogawa, Masashi Eguchi, Kazunori Toda

Scientific Research Section, GIKEN LTD.

Some of the IPA events in Kochi this July were held in the newly opened facility of GIKEN "RED HILL 1967" (GIKEN, 2023). This facility is mainly composed of an exhibition area showing the real-scale "Implant™" structures constructed by the press-in method and two innovative buildings of steel sheet piles, and provides a variety of information on a "seeing is believing" basis. This article will briefly introduce some examples of the researches on these structures, conducted by the research team in GIKEN or by other researchers. Please note that it does not provide a comprehensive review of related research on each structure.

1. Implant Bell Cap Bridge – a bridge on a hatted tubular pile constructed with special press-in piling system

The "Implant Bell Cap Bridge" is a bridge utilizing the "hatted tubular pile" (Fig. 1) as its pier pile and securing the bridge function by settling the deck panels on the hatted tubular piles via the T-shaped beams, constructed by a special press-in construction system (Fig. 2). The hatted tubular pile consists of an open-ended tubular pile (a "pile part") and a bell-shaped cap (a "hat part"), with the hat part being connected to the pile part near the ground surface. This bridge can be constructed in a small space within a short period, since (1) the construction system can be positioned and move on the bridge and (2) the embedment depth of the pier pile can be smaller than the conventional tubular pile due to the effect of the hat part. The construction procedure of the bridge is to (1) install the hatted tubular pile, (2) settle the T-shaped beam on the pier pile, (3) settle the deck panels on the T-shaped bars and (4) move the construction machine forward on the deck panels. The removal of the bridge can be conducted by following the reverse procedure.

The vertical and horizontal resistance of the hatted tubular pile were investigated by the 1-g model tests and full-scale field tests (Ishihara et al., 2016).

In the full-scale field tests, the static vertical and horizontal load tests were conducted on the tubular pile (with the outer diameter D_o being 0.8 m) and the hatted tubular pile (with D_o being 0.8 m and the outer diameter of the hat part being 2.2 m). The hat part was rigidly connected to the pile part. The embedment depths of the tubular pile and the hatted tubular pile were 4.4 m and 4.7 m respectively.

The vertical load displacement curves obtained in the field tests are shown in Fig. 3. The vertical capacity of the hatted tubular pile was around 1.7 times greater than that of the tubular pile, if the capacity was defined as the resistance at the base displacement of 1/10 of D_o. One of the mechanisms to increase the vertical capacity of the hatted tubular pile was expected to be the increase in the soil stress beneath the hatted part and the subsequent increase in the shaft resistance of the pile part. This mechanism was investigated in the field test by comparing the axial stresses of the pile part or the tubular pile at several levels, but was not clearly observed. The initial vertical stiffness (when the base displacement was smaller than 1/100 of D_o) was comparable in the hatted tubular pile and the tubular pile. This was thought to be because a certain displacement was necessary to achieve the fully plugged condition of the hat part and the full mobilization of the strength of the

Fig. 1. Hatted tubular pile

Fig. 2. Press-in construction system for the Implant Bell Cap Bridge
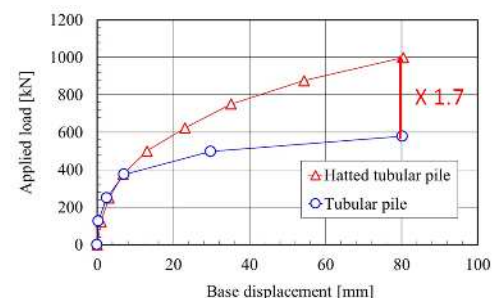
Fig. 3. Results of full-scale vertical load tests (after Ishihara et al. (2016))

soil beneath the hat part.

The horizontal load displacement curves obtained in the field tests are shown in Fig. 4. The horizontal capacity, defined as the resistance when the horizontal displacement of the pile at the ground surface level reached 15 mm, of the hatted tubular pile was around 1.5 times greater than that of the tubular pile. The initial horizontal stiffness of the hatted tubular pile was also greater than that of the tubular pile.

2. Confined Ground Seismic Damper – aseismic technology using a pressed-in sheet pile wall with a closed shape

The "Confined Ground Seismic Damper" consists of a pressed-in sheet pile wall with a closed shape and the ground confined by the wall. As exemplified in Fig. 5, it can be used beneath the structure (Fig. 5a) or as a structural component of the whole structure (Fig. 5b). It is expected to reduce the displacement of the structure due to the liquefaction of the ground, by preventing or mitigating (1) the sliding failure of the soil, (2) the deformation of the soil inside the wall, (3) the lateral movement of the liquefied soil, (4) the transmission of the excess pore water pressure and (5) the uneven settlement of the structure. It is also expected to provide a seismic damping function, by taking advantage of its structural flexibility in the liquefied ground.

As for the effectiveness for reducing the settlement and the inclination of the structure due to liquefaction, Kato et al. (2014) carried out 1-g model tests, centrifuge model tests and numerical analyses. The house models having the uneven load (Fig. 6) were used, with the sheet pile wall being connected to the spread foundation of the house. The ratio of the embedment length of the sheet pile wall to the thickness of the liquefiable layer (embedment ratio, z_{emb} / H_{liq}) was varied. The results are summarized in Fig. 7. When the embedment ratio was 1, the settlement and the inclination of the house were reduced by 90 % and 80 % respectively, as compared with the house having no sheet pile wall. In addition, the settlement and the inclination were confirmed to be reduced even when the embedment ratio was smaller than 1.

Toda et al. (2022, 2023) and Haigh (2022) conducted a series of 1-g large-scale model tests to investigate the vertical and horizontal resistance of the slab with a square sheet pile wall in a liquefiable ground. The tests were conducted using a soil tank shown in Fig. 8, where the liquefaction of the ground (the reduction of the effective stress) is simulated by using the seepage force generated by the water injection at the bottom of the soil tank (Ogawa et al., 2018). The extent of liquefaction was judged by the excess pore water ratio (r_u). The static vertical and horizontal load tests were conducted, with r_u being controlled constant during the tests either at 0, 0.3 or 0.6. Both the vertical and horizontal resistance were found to be smaller in the tests with larger r_u values. If plotted against r_u as shown in Fig. 9, both the vertical and the horizontal capacity were found to vary roughly linearly with r_u. These trends were consistent with those found for the single closed-ended tubular pile (Willcocks, 2021). These findings would be suggesting that the resistance of these structures in a liquefied ground could be estimated from their resistance in a non-liquefied ground.

Haigh (2022) conducted centrifuge tests and numerical analyses to
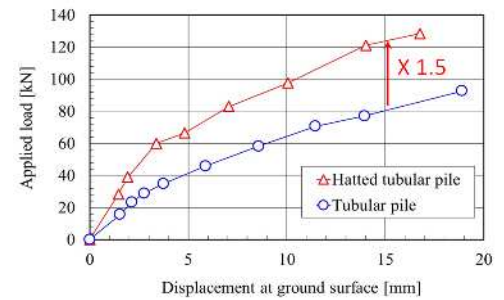
Fig. 4. Results of full-scale horizontal load tests (after Ishihara et al. (2016))

(a)

(b)
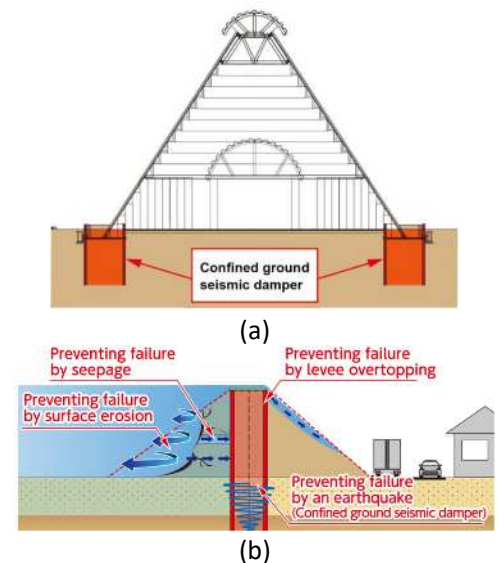
Fig. 5. Application examples of Confined Ground Seismic Damper (GIKEN (2023))
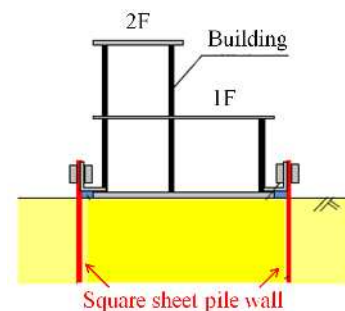
Fig. 6. House model used in the model test (after Kato et al. (2014))
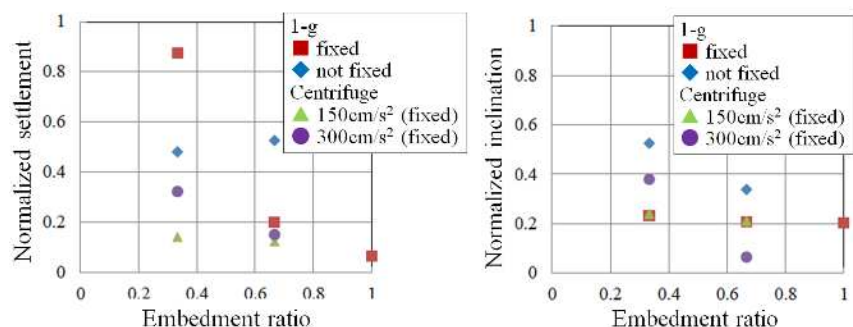
Fig. 7. Experimental results on the effect of square sheet pile wall on reducing settlement and inclination of house due to liquefaction (Kato et al. (2014))
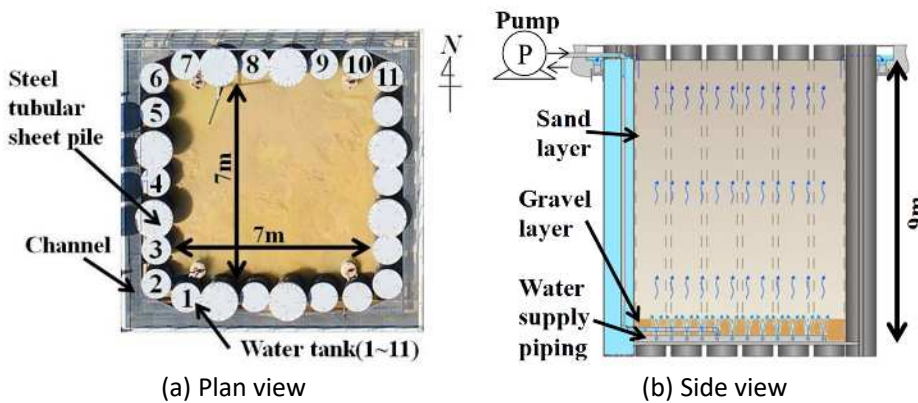
(a) Plan view
Fig. 8. Large-scale test apparatus for liquefaction (Ogawa et al. (2018))

(b) Side view
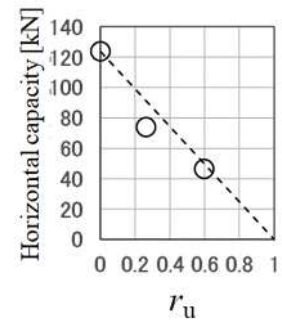
Fig. 9. Horizontal capacity vs. r_u (after Toda et al. (2023))

investigate the vertical and horizontal resistance of the same structure as was treated in the above-mentioned large-scale model tests, by applying a 0.36 g seismic loading to the model. She showed that a column of non-liquefied soil is created in and beneath the sheet pile wall a s shown in Fig. 10, and suggested that this will be one of the mechanisms for the structure to exhibit some resistance in a liquefied ground.
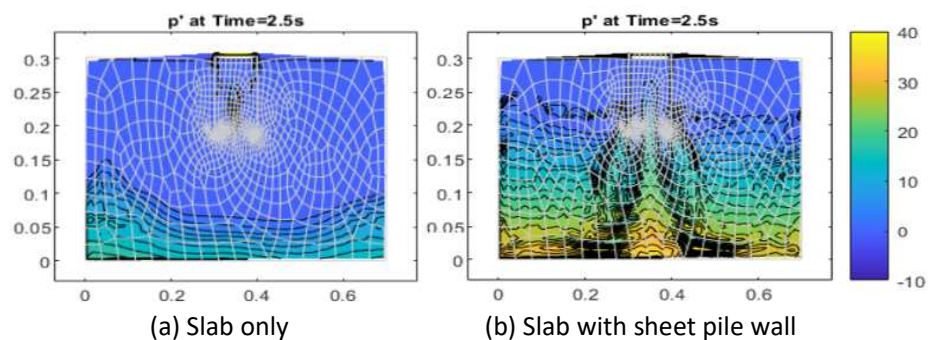
(a) Slab only   (b) Slab with sheet pile wall
Fig. 10. Results of numerical analysis (in kPa) (after Haigh (2023))

3. Preload Retaining Wall – a preloaded retaining wall consisting of steel sheet piles

The "Preload Retaining Wall" is a retaining steel sheet pile wall having an inclination angle and a bow shape. As shown in Fig. 11, the construction procedure of this wall is to (1) install the sheet piles by the press-in method at a certain inclination angle, (2) excavate one side of the wall, (3) apply a horizontal load (Preload) to the wall in its head, (4) fill the gap behind the wall with a backfill material and (5) remove the Preload.

Gao (2014) and Ishihara et al. (2015) conducted 1-g model tests and field tests to compare the deformation of a normal wall (a retaining sheet pile wall having no inclination), a slanting wall (a retaining sheet pile wall having an inclination angle of 5 degrees) and the Preload Retaining Wall having the same inclination angle with the slanting wall, when a
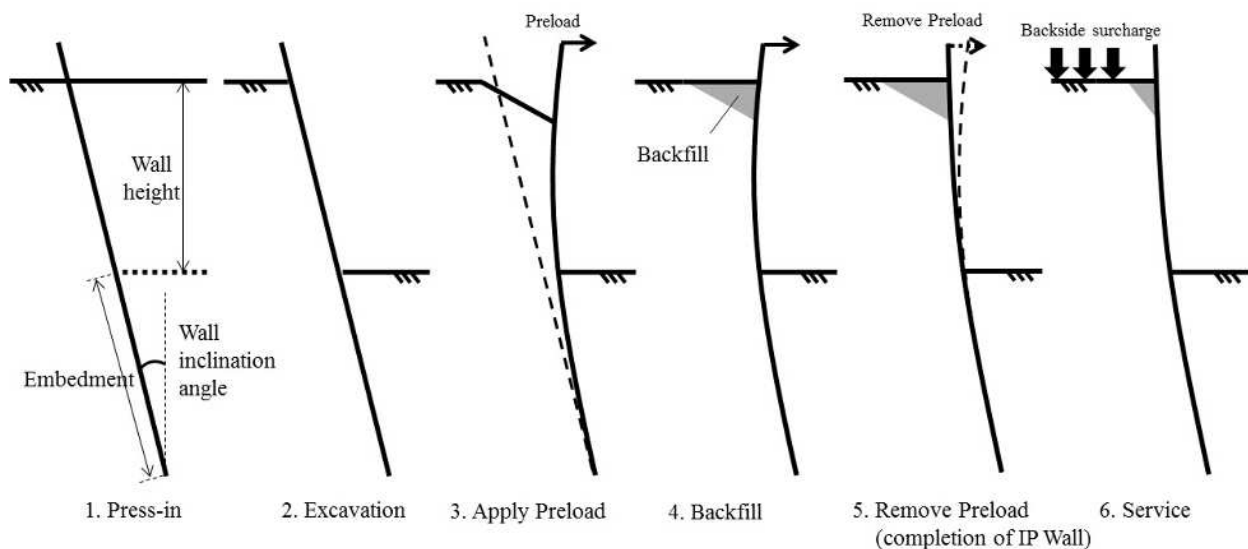
Fig. 11. Construction procedure of Preload Retaining Wall (Ishihara et al. (2015))

backside surcharge was applied behind each wall. The results are illustratively summarized in Fig. 12. The horizontal displacement caused by the surcharge of 20 kPa was smaller in the Preload Retaining Wall than in the slanting wall, by 99 % at the wall head and 74 % for the entire wall. The deformation pattern of the Preload Retaining Wall was different from that of the slanting wall. The maximum horizontal displacement was found near the excavation bottom in the Preload Retaining Wall, while it was found in the wall head in the slanting wall.

Ishihara et al. (2015) conducted numerical analyses to investigate the mechanisms for the smaller deformation of the Preload Retaining Wall confirmed in the field tests. They suggested based on the analysis results that the possible mechanisms were (1) the enhanced stiffness of the soil in the excavation bottom as a result of the loading history due to the Preload and (2) the improved shear strength of the backside soil as a result of the increased horizontal stress due to the elastic reaction of the steel sheet pile wall to the Preload, as summarized in Fig. 13.

A simple method to determine the amount of Preload was proposed by focusing on the first of the above-mentioned two mechanisms (Ishihara et al., 2015). The appropriate amount of Preload was assumed to correspond to the amount of the surcharge to be experienced in service, in terms of the effect on the soil in the excavation side. A conceptual two-dimensional diagram was introduced as shown in Fig. 14, where the effect of the Preload or the surcharge is expressed by the combination of the horizontal load and the moment at and around the cross point of the wall and the excavation bottom (in the vertical axis), while the deformation of the soil in the excavation side is represented by the summation of the horizontal displacement of the wall below the excavation bottom (in the horizontal axis).

4. Implant Barrier – a protective wall consisting of strut members (steel tubular piles) and wall members (concrete, metal, fiber etc.)

The "Implant Barrier" is a protective wall to be used for the disaster prevention and mitigation, by reducing the hydrodynamic load of tsunamis, wave surges and so on. As shown in Fig. 15, it mainly consists of the strut members (steel tubular piles) and wall members (made of concrete, metal or fiber). The strut members are aligned with a certain distance with each other, by being installed into the ground by the press-in method. The wall members are made either of concrete, metal or fiber, and are fixed to the strut members. The structural stability of the Implant Barrier is supposed to be assured by the strut members and optionally by the sheet piles.

The wall members of the Implant Barrier (hereinafter called "Barrier") can be porous sheets made of fiber. In this case, the reduction of the hydrodynamic load will be achieved by the energy loss of the flow when it passes through the Barrier. Suzuki et al. (2016) proposed a theoretical approach shown in Fig. 16 to consider the energy loss of the flow by introducing the "loss factor" (η), defined by $\eta = f / \lambda^2$ where f is the friction factor and λ is the aperture ratio of the Barrier. They confirmed its validity by conducting a series of two-dimensional hydraulic model tests in the apparatus shown in Fig. 17, using a surge-type tsunami. As shown in Fig. 18, the estimated and the measured tsunami load on the Barrier (F_B) and the flowrate of the tsunami after passing
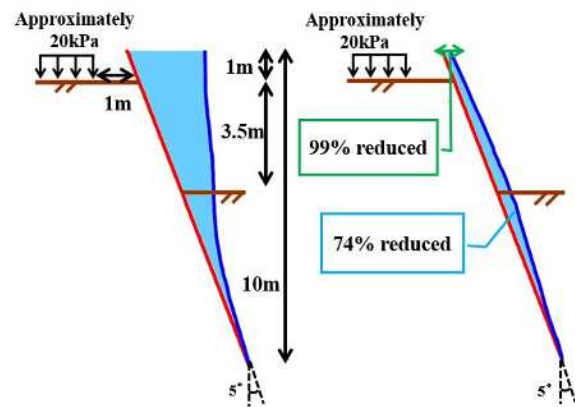
(a) Slanting wall   (b) Preload Retaining Wall
Fig. 12. Field test results (Ishihara et al. (2015))
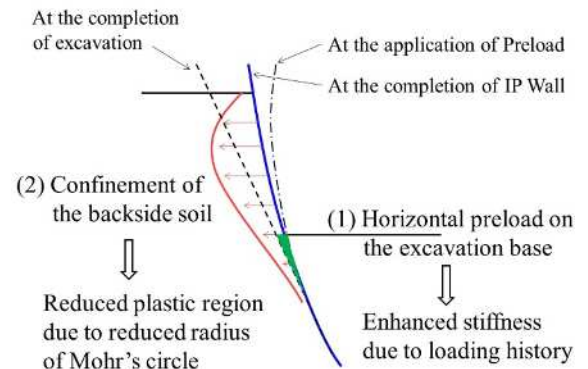
Fig. 13. Mechanisms of smaller deformation of Preload Retaining Wall (Ishihara et al. (2015))
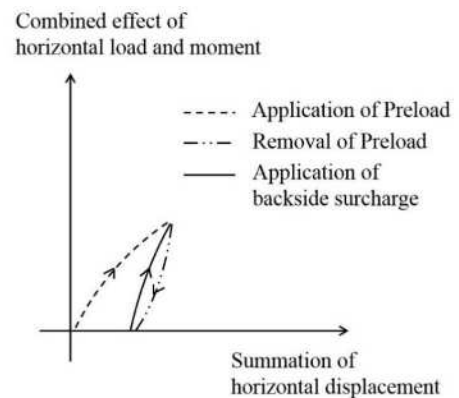
Fig. 14. Conceptual diagram for design of Implant Preload Wall (Ishihara et al. (2015))
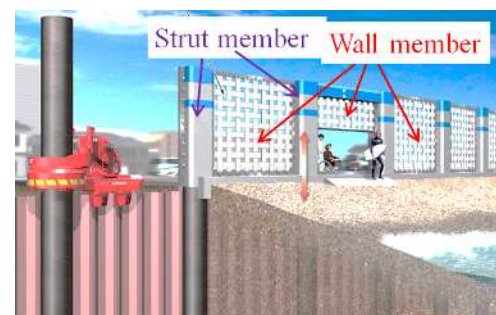
Fig. 15. Basic structure of Implant Barrier (after GIKEN (2023))
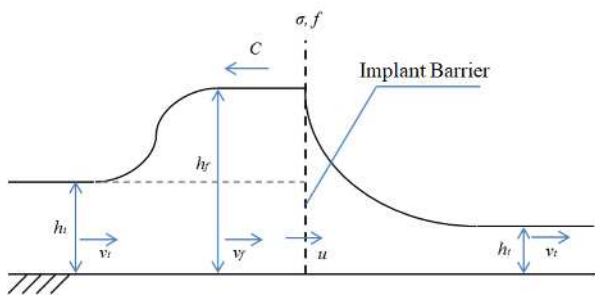
Fig. 16. Theoretical approach for Implant Barrier
(after Suzuki et al. (2016))
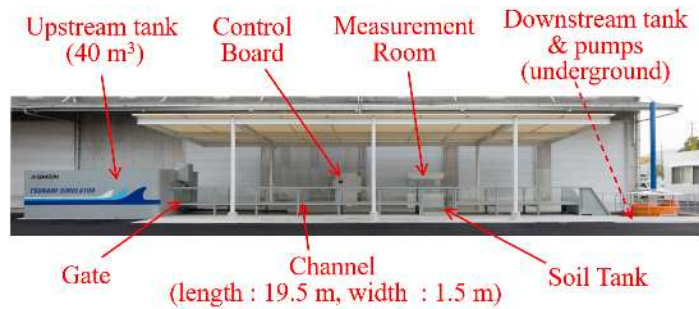
Fig. 17. Experimental apparatus to simulate tsunami
(after Ishihara et al. (2018))
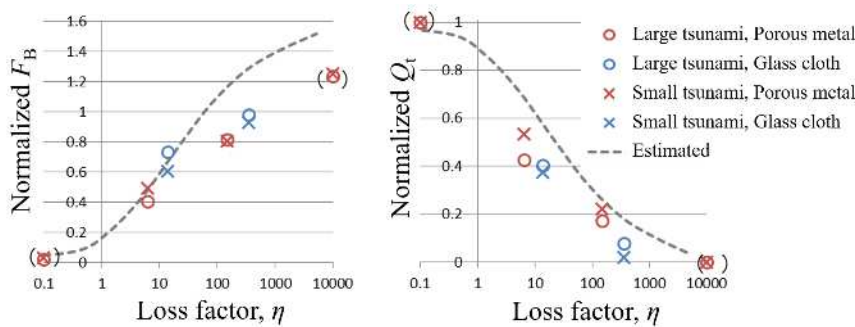
Fig. 18. Experimental results in comparison with estimated results
(after Suzuki et al. (2016))
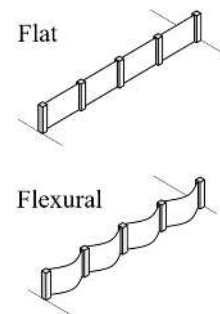
Fig. 19. Shapes of wall members
(after Toda et al. (2021))

the Barrier (Q_t) were confirmed to agree with each other to some extent, if tsunami did not overflow the Barrier. A trade-off relationship was confirmed between F_B and Q_t with regard to the loss factor η, where increasing the η value (i.e. reducing the aperture ratio λ) led to greater F_B and smaller Q_t values. In addition, an experimental method to obtain η was also introduced to cope with the difficulty in defining the λ value of the porous sheet made of fiber.

Toda et al. (2021) proposed a method to apply the theoretical approach of Suzuki et al. (2016) to the tsunami overflowing the Barrier, by introducing the "equivalent aperture ratio" and the "equivalent loss factor". Its validity was assessed by comparing with the results of the hydraulic model tests conducted in the same apparatus. As a result, the water depth behind the Barrier was well estimated, while the water depth in front of the Barrier and the tsunami load on the Barrier were underestimated.

Toda et al. (2021) also investigated the effect of the shape of the wall members of the Barrier (flat or flexural, as shown in Fig. 19) on reducing the tsunami load behind the Barrier (F_D), by using the porous sheet made of fiber for the wall members. They confirmed that the flexural shape was slightly more effective. For example, the Barrier with λ = 24 % was confirmed to reduce F_D by 75 % if the wall members were flat and by 80% if they were flexural.

References

Gao, G. 2014. Comparing performance of different sheet pile walls. M.Eng. Thesis, University of Cambridge, 50p.

GIKEN. 2023. GIKEN RED HILL 1967, Akaoka Kochi, Japan. https://redhill1967.giken.com/en/

Haigh, A. 2022. Performance of Implant structures. M.Eng. Thesis, University of Cambridge, 52p.

Ishihara, Y., Ogawa, N., Okada, K. and Kitamura, A. 2015. Implant Preload Wall: a novel self-retaining wall with high performance against backside surcharge. Press-in Engineering 2015, pp. 68-82.

Ishihara, Y., Ogawa, N., Okada, K., Inomata, K., Yamane, T. and Kitamura, A. 2016. Model test and full-scale field test on vertical and horizontal resistance of hatted tubular pile. Proceedings of the Third International Conference Geotec Hanoi 2016 - Geotechnics for Sustainable Infrastructure development, pp. 131-139.

Kato, I., Hamada, M., Higuchi, S., Kimura, H. and Kimura, Y. 2014. Effectiveness of the sheet pile wall against house subsidence and tilting induced by liquefaction. Journal of Japan Association for Earthquake Engineering, Vol. 14, No. 4, pp. 35-49. (in Japanese)

Ogawa, N., Ishihara, Y., Ono, K. and Hamada, M. 2018. A large-scale model experiment on the effect of sheet pile wall on reducing the damage of oil tank due to liquefaction. Proceedings of the First ICPE 2018, Kochi, pp. 193-202.

Suzuki, N., Ishihara, Y. and Isobe, M. 2016. Experimental study on influence of porosity and material of pile-type porous tide barrier on its tsunami mitigation effect. Journal of Japan Society of Civil Engineers, Ser. B3 (Ocean Engineering), Vol. 72, No. 2, pp. I-491-I-496. (in Japanese)

Toda, K., Mori, A., Ishihara, Y. and Suzuki, N. 2021. Experimental study on tsunami mitigation effect of pile-type porous

tide barrier. Proceedings of the Second International Conference on Press-in Engineering 2021, Kochi, pp. 444-453.

Toda, K., Ishihara, Y., Eguchi, M. and Mori, A. 2022. Experimental study on a foundation reinforced by square sheet pile wall. Japan Society of Civil Engineers 2021 Annual Meeting, 2p. (in Japanese)

Toda, K., Ishihara, Y., Eguchi, M. and Mori, A. 2023. Horizontal resistance of a slab reinforced by square sheet pile wall in a liquefied ground. Japan Society of Civil Engineers 2023 Annual Meeting, 2p. (in Japanese)

Willcocks, F. 2021. The vertical and horizontal performance of pressed-in tubular piles in liquefied ground. M.Eng. Thesis, University of Cambridge, 52p.